Journal of the Korean Society of Marine Engineering, Vol.31, No.7, pp. 842~851, 2007(ISSN 1226-9549)

Characteristics of Vortical Jet Structures of a Hydrofoil

Chang-Jo Yang† · You-Taek Kim* · Min-Seon Choi**

(Manuscript : Received April 27, 2007 ; Revised August 23, 2007)

Abstract : Oscillating foil propulsion, the engineering application of fish-like movement of a hydrofoil, has received in recent decades as a possible competitor for propellers. The oscillating foil produces an effective angle of attack, resulting in a normal force vector with thrust and lift components, and it can be expected to be a new highly effective propulsion system. We have explored propulsion hydrodynamics as a concept in wake flow pattern. The present study has been examined various conditions such as oscillating frequencies and amplitudes in NACA0010 profile. Flow visualizations showed that high thrust was associated with the generation of moderately strong vortices, which subsequently combine with trailing-edge vorticity leading to the formation of a reverse Kármán vortex street. Vortex generation was inherent to jet production and playeda fundamental role in the wake dynamics. And it was shown that the strong thrust coefficient obtained as the Strouhal number was larger.

Key words : Heaving foil, PIV, Reverse Kármán vortex street, Vortex center, Jet, Propulsion

1. Introduction

Fish swimming hydrodynamics has captured the interest of many researchers for centuries. Long years of evolution have produced more than 22,000 species of fishes. Despite remarkable individual species evolutions, most fishes swim using similar motions. Consequently, it is well accepted that fishes have evolved to efficiently propel themselves through water. Fish swimming has been studied for many years by biologists as well as many fluid mechanicists[1]-[3]. Fishes are able to propel themselves for great distances and accelerate and maneuver.

Oscillating foil propulsion, the engineering application of fish-like movement of a hydrofoil, has received in recent decades as a possible competitor for propellers. The oscillating wing has pitch and heave motions made possible by adopting two or more locomotive hinges arranged parallel to the wingspan. Thus, the wing can produce a propulsive force as well as a lifting force over the whole span of the wing. High efficiencies, comparable to and exceeding those of typical screw

† Corresponding Author(Dept. of Marine Systems Engineering, Mokpo National Maritime University), E-mail:cjyang@mmu.ac.kr, Tel: 061)240-7085
* Dept. of Marine Systems Engineering, Korea Maritime University
** Dept. of Marine Systems Engineering, Mokpo National Maritime University

propellers have been reported in the literature[4]-[5]. Large amplitude foils oscillated at the correct frequency can provide significant thrust levels very efficiently. The premise has many exiting engineering application such as ship propulsion, maneuvering and flow control.

It has been known for many decades that fishes produce a highly vortical jet wake. Kármán and Burgers[6] first introduced the conception that the famous Kármán vortex street can also work in reverse, generating thrust instead of drag. This average jet flow is unstable with a narrow range of frequencies of amplification. The unsteady fluid mechanism is characterized by the formation of a strong vortex on the surface around the foil. The interaction between the unsteady vortices shed by the foil and inherent dynamics of the unstable wake results in the formation of patterns of large-scale eddies. Moreover, the formation of vortices in the wake of the oscillating foil is closely associated with the propulsive efficiency and can identify by tracking centers of these vortices. The objective is therefore to investigate the unsteady effect and the dynamics of the trailing edge vortex to unfold the basic mechanism which generates foil propulsion. In this paper we deal with oscillating motion as pure heave motion of a foil while translating forward.

Meanwhile, some progress has been made by these studies in analyzing the characteristics of vortices, but the topological structure and their relationships to the thrust generation in the near wake still remain obscure to us. Moreover, most of previous experimental approaches to these structures have been made using flow visualization and point measurements. In qualitative visualization, however, the presence of discrete vortices merely based on the rolling-up of the streaklines cannot be positively identified. Particle image velocimetry[7] has emerged into a powerful alternative to the previous point-wise and time-mean velocity measurement technique as laser doppler velocimetry and hot-wire anemometer.

To investigate the vortex dynamics, which is crucial to the force generation on the heave foil, experiments therefore were performed in circulating water channel using the technique of PIV system based on the two-frame gray level cross correlation method. As results, it was reported that the heaving motion over a certain Strouhal number makes the reverse Kármán vortex street in the wake. The overall features of the unsteady vortex dynamics also have been investigated.

2. Experimental Apparatus and Procedure

Fig. 1 shows the experimental apparatus. Experiments were conducted on a NACA 0010 foil with chord equal(c) to 0.06 m and span(l) 0.2 m, fitted with circular end plates to ensure two-dimensional flow and to reduce end effects. The flow generation system was a circulating water tunnel and main flow velocity was 0.067 m/s. The water channel had the following dimensions: 0.675 m (L)× 0.3 m (H)× 0.35 m (D). A TBVST(Termi-BUS Module) unit digitally controlled Ternary DC servo Motor (RMJ0711, Dyadic systems Co., Ltd) and a lead-screw table provided the means

for heaving the foil. The size of the analyzed region was 0.2 m × 0.1 m.

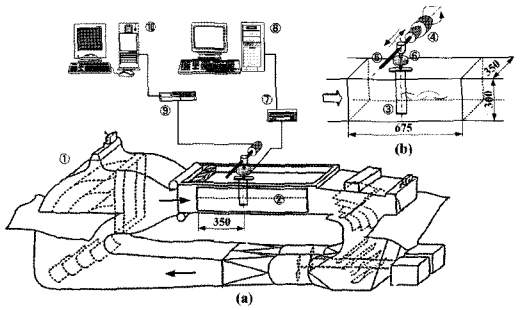

① Water tunnel ② Test section
③ NACA 0010 ④ DC servo motor
⑤ Ball screw ⑥ 6-axis force sensor
⑦ Motor driver ⑧ Motor controller
⑨ A/D board ⑩ PC

Fig. 1 Experimental apparatus

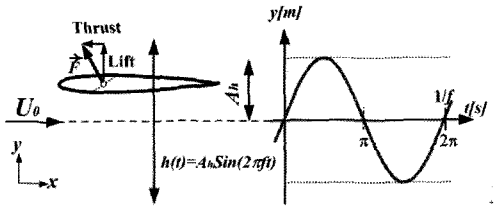

Fig. 2 Trajectory of the oscillating foil

For illuminating the flow field of thePIV experiment, a 4W water-cooled Argon-Ion laser with a fiber optic assembly generates a two-dimensional thin sheet light of about 2 mm thickness. Orgasal particles with mean diameter 50 m and specific weight 1.1 g/cm^3 are seeded. The scattered light is captured by a high-speed camera (Phantom V5.0, Phantom) with a large internal memory block. This camera has an 8-bit sensor array of 1,024× 1,024 pixels and can obtain images at a maximum speed of 1000 frames/sec with full resolution and 62,500 frames/sec with partial resolution. The large internal memory block (1,024MB) allows 1,024 frames at full resolution to be saved successively. Phase difference between two images for cross correlation influences the accuracy of phase resolution. The smaller phase difference between two images becomes the more the accuracy of phase resolution increases. Maximum phase difference between two images for cross correlation was therefore set to under 2[pixel]. A spatio-temporal resolved PIV system, which can be achieved to increase the spatial resolution and dynamic range of detecting particle image displacements in PIV images, was adopted. As steps for the post processing, error removing, reallocation in grid and conversion of pixel to real unit procedures were performed. The divergence criterion satisfying the continuity equation was adopted in the error removal procedure. Error uncertainty by the automated procedure was on the average less than 2 % in the vector identification. In the present study, the phase detection is based upon the DC servo motor pulse signal and the streamwise velocity signal. And thus, the phase average was realized by taking an average over the conditional sampling at a given phase. To accurately estimate the vorticity defined in terms of the velocity gradient, an adaptive scheme coupled with a least squares second-order polynomial at different grid spaces was adopted to minimize the total error which is defined as the summation of the experimental and truncation errors[8].

To investigate the unsteady fluid forces and associate them to visualization results, the forces acting on the heaving foil were measured. The unsteady fluid forces were measured with a mini 6-axis

force sensor (Mini 2/10, BL Autotec), placed at one end of the foil attachment, which is based on the principle of pressure pick-up device and characterized by simple structure and miniature size.

A single heaving motion was imposed with various combinations of heaving frequency, f and amplitude, A. Fig. 2 shows the trajectory of the heaving foil. The solid line is the heaving waveform ($h(t)=A\cdot\sin 2\pi ft$). The non-dimensional frequency, called Strouhal number is defined as $St = f\cdot 2A/U_0$, where U_0 denotes the free-stream velocity. Note that St measures the ratio of the heaving velocity and the mean forward velocity. Experiments were conducted with the Strouhal numbers between 0.0 and 0.9, while an intense investigation was also made for the effect of a neutral wake structure, where a pair of vortices with different rotating velocity stood in a line.

3. Results and Discussion

3.1 Temporal distribution of velocity field and time-averaged velocity profiles

PIV measurements were conducted at the Reynolds number, $Re=4.0\times 10^3$. Fig. 3

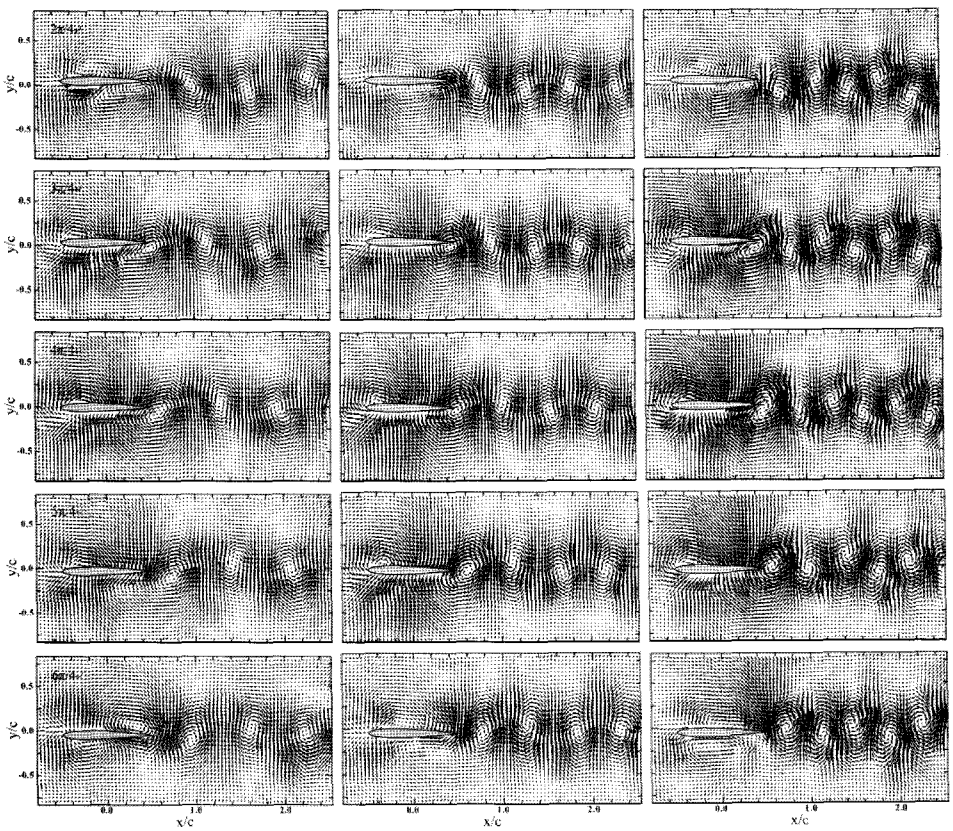

(a) St = 0.06 (b) St = 0.07 (c) St = 0.11

Fig. 3 Development of the trailing-edge vortex during the shedding process (Down-stroke): The corresponding phases are 2π/4, 3π/4, 4π/4, 5π/4 and 6π/4 from the top

shows the development of trailing-edge vortices as the foil is oscillated (down-stroke) in heave with amplitude A/c= 0.04 for f = 0.8, 1.0 and 1.5. These conditions correspond to the Strouhal number of 0.06, 0.07 and 0.11. The corresponding phases are $2\pi/4$, $3\pi/4$, $4\pi/4$, $5\pi/4$ and $6\pi/4$ from the top. Here, the flow is from left to right. Fig. 3(a) shows vortex flow patterns at St = 0.06. At a relatively low Strouhal number the wake structures consist of clockwise rotating vortices in the upper row and counter-clockwise rotating vortices in the lower row. Induced flow has a component moving backward with respect to the foil to generate the drag. The shedding of two vortices per cycle was formed that carries the Kármán vortices similar to those observed by Williamson[9]. For St 〈0.06, the wake does not roll up into discrete vortices and retains its wavy forms.

In the case of Fig. 3(b), the increase of the Strouhal number places the vortices centers on a line. Well-organized vortices are present, while pairs of vortices are shed in the wake. The alternating vortices are positioned almost in the same line and indicate the typical neutral structure, which yields zero force when averaged over one period of oscillation.

A strong trailing-edge vortex forms and

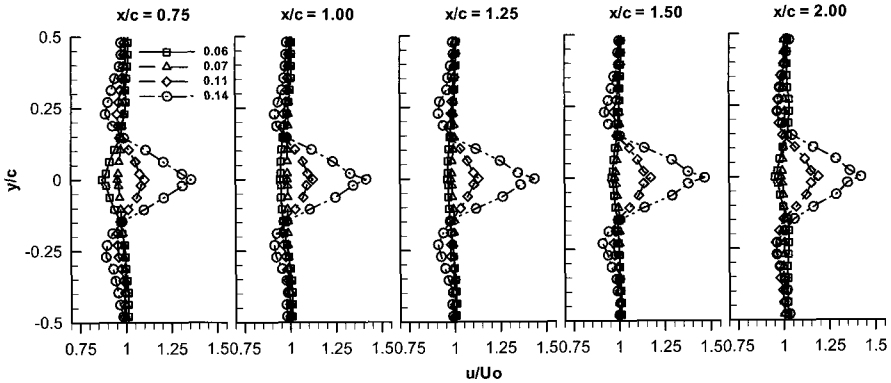

(a) Streamwise velocity profiles

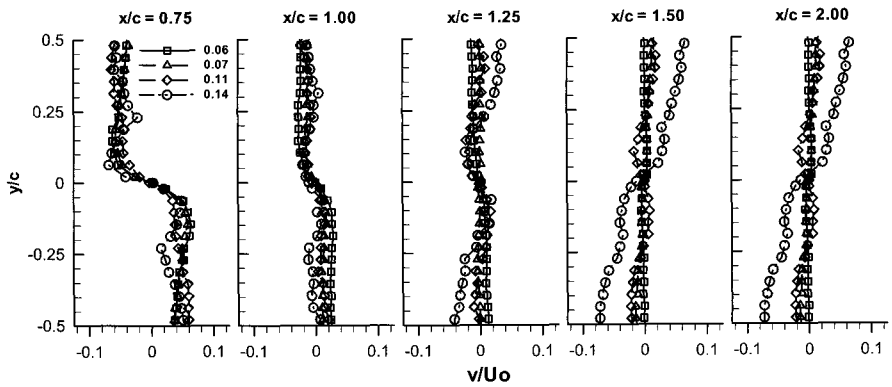

(b) Cross-stream velocity profiles

Fig. 4 Comparison of time-averaged velocity profiles

is shed well just after the foil reaches the zero amplitude excursion in Fig. 3(c), while the wake consists of two vortices per cycle. At a sufficiently high Strouhal number the upper row of vortices are counter-clockwise rotating (positive circulation) while the lower row of vortices are clockwise rotating (negative circulation). Especially, a reversed flow pattern was generated in comparison with Fig. 3(a). This structure is revere Kármán vortex street, which has opposite circulation and different strength. Jones et al.[10] and Yang et al.[11] have reported that the formation of the reverse Kármán vortex street is closely associated with the vortex structure of thrust production.

Fig. 4(a) shows time-mean streamwise velocity profiles. Mean velocity profiles were measured 0.75c, 1.00c, 1.25c, 1.50c and 2.00c downstream of the center of the foil in various Strouhal numbers. Variations during oscillations were obtained by averaging long-time velocity data behind the heaving foil. The averaged wake profiles are different at each Strouhal numbers due to the changes in force and momentum integral around the foil. As the Strouhal number increases (St $>$ 0.07), it can be seen that the wake profiles with velocity deficit can be transformed into the wake with velocity excess(jet). Because velocity perturbations close to the wake centerline are advected downstream more quickly than the more off-centered parts in jet. The wake structure therefore has the form of a jet, which shows the reverse Kármán wake accompanied by the interaction between vortices shed by the foil and innate dynamics of the wake. In the case of St = 0.07, the mean velocity profile shows that a condition exists that the wake has no velocity deficit and excess. This condition occurs when the alternating vortices are positioned on the nearly straight line as shown in Fig. 3(b).

Meanwhile, Fig. 4(b) shows time-mean cross-stream velocity profiles. It can be seen that the transverse wake profiles are rotated in a counter-clockwise direction and they eventually switch their signatures as the Strouhal number increases. This is because v-component velocities are advected adversely in cross-stream, which switch vortex formation in the wake as shown in Fig. 3. This will be discussed with temporal evolutions of the shedding vorticity and trajectories of vortex center

3.2 Trajectories of vortex center

Fig. 5 shows trajectories of the streamwise and cross-stream positions of vortex centers, where two procedures to detect vortex centers are compared. Each symbol represents the position of the vortex center every 1/30 sec. All symbols in all figures are acquired in down-stroke. Note that the peak positions obtained from the instantaneous flow field are more scattered than those obtained from the averaged flow field at constant phase. The scattering of the data from the peak position of the vorticity seems to be caused by the vortex separation and the local-peak movement. The positions obtained from the centriod of the vorticity field are more continuous then positions by finding the peaks of the vorticity. Since a vortex can be thought as a rotational flow, it seems reasonable to assume the centroid

of vorticity to be the center of rotation. The Max. RMS error between the instantaneous and phase-averaged data identified based on the centriod of the vorticity field results to 1.3% for streamwise locations and 4.5% for cross-stream locations.

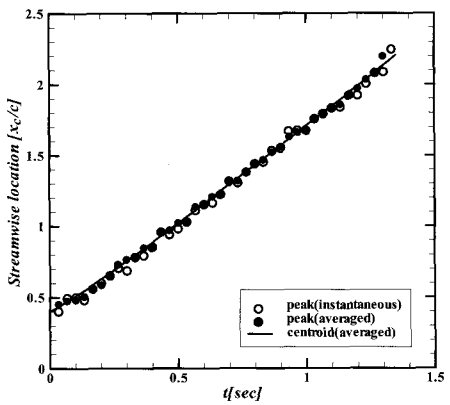

(a) Streamwise locations

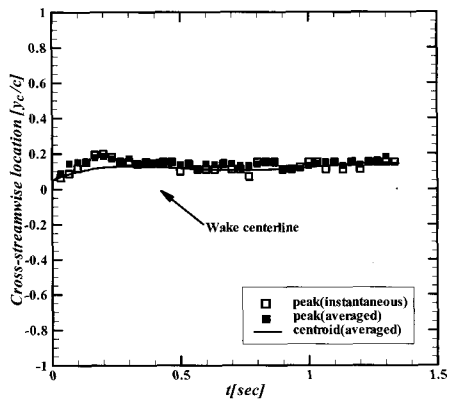

(b) Cross-stream locations

Fig. 5 Comparison of trajectories of the vortex center identified (St = 0.23).

Fig. 6 shows the streamwise and cross-stream locations of the vortex center identified based on the centriod of the vorticity field at different Strouhal numbers in the downstream region. It can be seen that streamwise locations of the vortex centers in Fig.6 (a) move downward fast as increasing of the Strouhal number. Interestingly in Fig.6(b), apart from the separating shear layers to the oscillating foil, the trailing-edge vortex is moved upward in down-stroke at the rear of the foil as the Strouhal number increases. This is important because the shed vortices are switched in the wake and make the reverse Kármán vortex street.

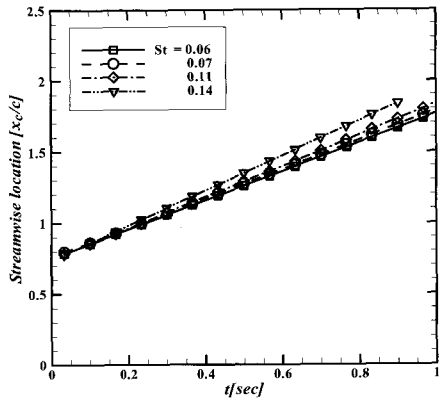

(a) Streamwise locations

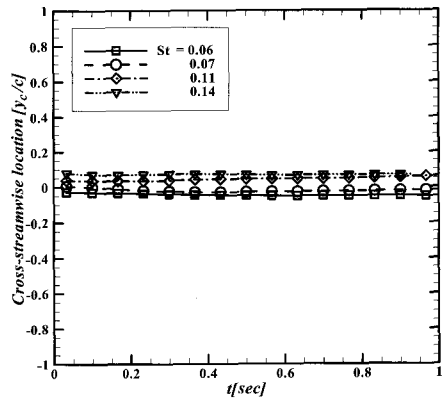

(b) Cross-stream locations

Fig. 6 Streamwise and cross-stream locations of the vortex center at different Strouhal numbers.

3.3 Estimation of thrust force

The drag or thrust generated by a body can be predicted by measuring the

momentum deficit or excess downstream of the body. The mean velocity profile u(y) can use to estimate the mean streamwise force on the foil. If we assume that the average flow is steady and incompressible and that the pressure is constant along the control volume boundaries, that is, the dowmstream pressure is equalized to the free stream value, the thrust on the foil T can be written in terms of the flux of momentum in the x-direction as

$$T = \rho \int_{-\infty}^{\infty} u(y)(u(y) - U_0)dy \qquad (1)$$

where the contributions due to the time-fluctuating quantities and the pressure term have been neglected. The mean velocity profile is obtained from the present PIV experiment results. A negative value of Ct (= $T/(1/2)\rho c l U_0$) corresponds to drag and a positive value implies thrust.

In Fig. 7, thrust coefficients directly measured using the 6-axis sensor, estimated using the simplified momentum integral, Eq. (1) and calculated by the invisid linear analysis [12] are compared. Thrust coefficients are found to increase consistently with the Strouhal number. Thrust experimentally measured is less than that calculated by Garrick. This discrepancy can be expected because there is a viscous drag that does not exist in the invicid case. However, the measured thrust is larger than that estimated by momentum integral. This may be expected because the simplified momentum integral based on time-averaged velocity profiles and the thrust estimated from integration of mean streamwise velocity profiles would incur errors at high frequencies. Especially, the critical point, which transfers drag force to thrust, can be seen to exist in the vicinity of the Strouhal number, St = 0.07. It can be also seen that the highest thrust coefficient is obtained at the higher Strouhal number.

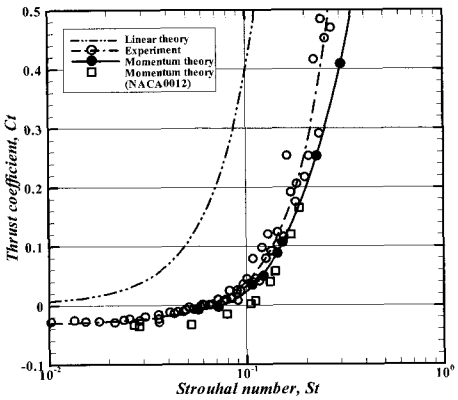

Fig. 7 Variation of thrust coefficient with the Strouhal numberl

4. Conclusions

PIV experiments were performed to investigate the vortex flow patterns of the heaving foil after parametric searches, which were added by a consideration of mechanisms governing the dynamics of its wake. The conclusions of the present study are enumerated in the following.

1) The experiments showed not only that thrust was feasible, but also that it was achieved a substantial thrust with only heaving motion. As the Strouhal number is greater than 0.07, wake profile with velocity deficit can be transformed into the wake with velocity excess.

2) Jet structure was investigated using tracking trajectories in temporal evaluation of the shed vortices, after

evaluating vortex center.

3) Flow visualizations showed that high thrust was associated with the generation of moderately strong vortices, which subsequently combine with trailing-edge vorticity leading to the formation of a reverse Kármán vortex street.

Further, we will report on the results of the authors' investigation of pitch motion, which are quite different from either of the results mentioned above.

References

[1] J. Gray, "Studies in Animal Locomotion 6. The Propulsive Powers of the Dolphin," Journal of Experimental Biology, Vol. 13, pp. 192-199, 1936.

[2] M. J. Lighthill, "Note on the Swimming of Slender Fish," Journal of Fluid Mechanics, Vol. 9, pp. 305-317, 1960.

[3] T. Y. Wu, "Hydromechanics of Swimming Propulsion," Journal of Fluid Mechanics, Vol. 46, pp. 337-355, 1971.

[4] G. S. Triantafyllou, M. S. Triantafyllou and R. Gopalkrishnan, "Optical thrust development in oscillating foils application to fish propulsion," Journal of Fluids and Structures, Vol. 7, pp. 205~224, 1993.

[5] J. M. Anderson, K. Streitlien, D. S. Barrett and M. S. Triantafyllou, "Oscillating airfoils of high propulsive efficiency," Journal of Fluid Mechanics, Vol. 360, pp. 41~72, 1998.

[6] T. von Kármán and J. M. Burgers, General Aerodynamic Theory Perfect Fluids, Aerodynamic Theory, (ed. W. F. Durand), Vol.2, Berlin-Springer, 1935.

[7] R. J. Adrian, "Particle-imaging techniques for experimental fluid mechanics," Annual Review Fluid Mechanics, Vol. 23, pp. 261~304, 1991.

[8] L. Lourenco and A. Krothapalli, "On the Accuracy of Velocity and Vorticity Measurements with PIV," Exp. Fluids, Vol. 18, pp. 421-428, 1995.

[9] C. H. K. Williamson, "Vortex dynamics in the cylinder wake," Annual Review of Fluid Mechanics, Vol. 28, pp. 477~539, 1996.

[10] K. D. Jones, C. M. Dohring and M. F. Platzer, "Experimental and computational investigation of the Knoller-Bentz effect," AIAA Journal, Vol. 36, No. 7, pp. 1241~1246, 1998.

[11] C. J. Yang, M. Fuchiwaki and K. Tanaka, "Propulsive Vortical Patterns and Unsteady Fluid Forces of a Flapping Airfoil," ASME Fluids Engineering Conference, FEDSM2003-45227, 2003.

[12] I. E. Garrick, "Propulsion of a Flapping and Oscillating Airfoil," NACA Rept. 567, 1936.

Author Profile

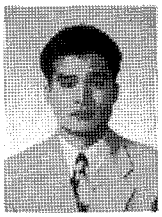

Chang-Jo Yang

He received his B.E. and M.E. degrees from Korea Maritime University, and his Ph.D. from Kyushu Institute of Technology, Japan. He is currently a professor in the Dept. of Marine System Engineering at Mokpo National Maritime University, Korea. His research interests are fluid machinery, flow visualization and CFD.

You-Taek Kim

He received his B.E. and M.Eng. degrees from Korea Maritime University, and his Dr.Eng. from Kyushu Institute of Technology, Japan. He is currently an associate professor in the Dept. of Marine System Engineering at Korea Maritime University in Busan, Korea. His research interests include fluid machinery, two-phase flow, cavitation, CFD.

Min-Seon Choi

He received his B.E., M.E. and Dr.Eng. degrees from Korea Maritime University. He is currently a professor in the Dept. of Marine System Engineering at Mokpo National Maritime University, Korea. His research interests include fluid machinery, measurement techniques for flow visualization.